Design of a 3-6 Hexapod Platform Sensor Using Forward Kinematics

Hongliang Shi, Yu She and Xuechao Duan

***Abstract*—This paper presents a design of a 3-6 hexapod platform for motion measurement. This hexapod platform is capable of determining the displacements in 6 degrees of freedom (DOF) by measuring the length changes of the struts. Based on the geometric layout, a kinematic modeling of the platform is described in this paper. The forward kinematics is derived for the mechanism to establish the relationship of the output and input: the displacements of the top platform, and the length changes of the struts. Based on the derived model, an algorithm of 6DOF motion measurement is proposed for the platform sensor based on two angle systems. A case study is presented for the discussion of the forward kinematics based measurement algorithm, and the application of the platform sensor.**

***Index Terms*—measurement algorithm, sensor, Stewart platform, hexapod, metrology, kinematics.**

I. Introduction

A parallel mechanism is formed by connecting a functional body to a reference body through two or more elements [1]. Parallel mechanism is widely used in motion positioning device with high precision. A lot of prior work by other researchers has been done regarding design, kinematic modeling of parallel mechanisms [2], [3], [4], [5]. Culpepper and Anderson [6] designed and calibrated a monolithic spatial compliant nano-manipulator. Chen and Culpepper [7] designed and calibrated a six-axis micro-scale nanopositioner. Dagalakis et al. [8] derived the kinematic model of a parallel robot link crane. Chao et al. [9] presented a novel method for kinematic calibration of a planar parallel flexure positioner. Varadarajan and Culpepper [10] conducted the calibration of a dual-purpose positioner-fixture, which has 6 degree-of-freedom (DOF). Shi et al. [11] did kinematic calibration of a hexapod nanopositioner. Chen and Hsu [12] derived the kinematic model of a tripod machine tool.

Although a lot of work has been done in design, manufacturing, and calibration of hexapod platform and parallel mechanisms [13], [14], there is little work on the design of parallel mechanisms for motion measurement. Olarra et al. [15] designed a hexapod mechanism, derived the kinematic models and did the calibrations. Nubiola and Bonev [16] built a 6DOF parallel measurement system. Nanua et al. [17] derived a kinematic model of a 3-6 Stewart platform. The modeling and measurement algorithm of the designs are critical for the accuracy in measuring 6DOF.

In this paper, we design a 3-6 hexapod platform for 6DOF displacement measurement. The platform sensor is capable of measuring the displacement of the top platform by means of the data of the struts lengths. A kinematic modeling is described based on the topology and geometric layout of the design. A forward kinematic solution is analyzed to build an algorithm of two situations for measuring the displacement of the top platform. Discussion and Comparison are proposed for guiding the use of the measurement algorithm.

The rest of the paper is organized as follows. Section II illustrates the design and the topology of the 3-6 hexapod platform. In Section III, we present the kinematic model of the platform. In section IV, the forward kinematics measurement algorithm is proposed for this motion sensor design, based on two angle systems. Section V is the case study and discussion of the forward kinematics based measurement algorithm. Section VI is the conclusion of the paper.

Manuscript received July 12, 2015; revised Aug 09, 2015.

Hongliang Shi is with the Mechanical Engineering and Aerospace Department, The Ohio State University, Columbus, OH 43210, USA. Corresponding author. (e-mail: shi.347@osu.edu).

Yu She is with the Mechanical Engineering and Aerospace Department, The Ohio State University, Columbus, OH 43210, USA.

Xuechao Duan is with Key Laboratory of Electronic Equipment Structure Design, Xidian University, China.

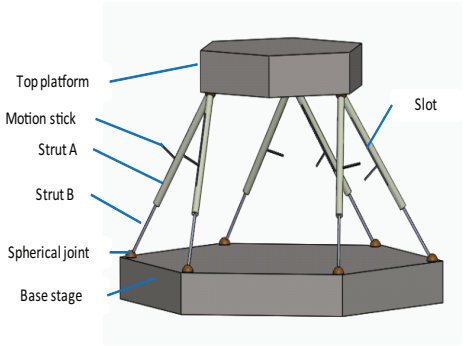

Fig. 1. Design of a 3-6 Hexapod Platform

II. Design of a 3-6 Stewart Platform

In this section, we present the design of a platform sensor based on the 3-6 Stewart Platform. The design principle and the topology of the platform are described.

A. Design of a 3-6 Stewart Platform

In order to obtain the displacement in 6DOF, we decide to use a hexapod design. The parallel Stewart Platform design has the advantage of high precision with limited workspace and is widely used in many applications. However, it is not efficient to obtain the solution of forward kinematics. In order to obtain the forward solution, we choose a 3-6 hexapod platform instead 6-6 hexapod platform. The struts are independent in 6-6 hexapod platform while each two struts are connected on the same top points in a 3-6 hexapod platform.

As shown in Fig. 1, the platform is composed of three main parts: base stage, struts, and top platform. The base stage is fixed to ground. The moving top platform is the load-carrying part, which is used as the end effector for measuring. The strut is composed of two separate segments defined as strut

ISBN: 978-988-19253-6-7
ISSN: 2078-0958 (Print); ISSN: 2078-0966 (Online)

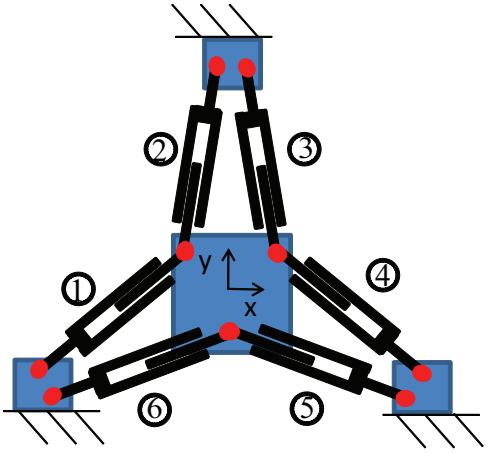

Fig. 2. Schematic Drawing of the Hexapod Platform.

A and strut B, shown in Fig. 1. Strut A is a tube with a long slot. One end of the strut A is installed with a spherical joint, which is connected to the top platform. Strut B is placed into strut A. One end of the strut is also installed with a spherical joint which is connected to the base stage. A motion stick of strut B is extruded from the slot of the strut A. The motion stick is used to attach translational displacement sensor.

B. Topology Analysis

As shown in Fig. 2, we build the global coordinate system on the top center of the top platform at the home position. The base stage is fully constrained in 6DOF. The struts are connected to base stage with six spherical joints. Bottom 6 spherical joints are independent between each other and each has 3DOF of rotation. The top platform is connected to 3 spherical joints. The six struts are connected in parallel to the top platform at the three joints. Each two struts are connected to one joint independently from each other. This means that each strut also has 3DOF at the top spherical joint. This setting can be considered as six independent spherical joints while each two joints geometrically overlap at the same place.

III. KINEMATIC MODEL

In this section, we illustrate the kinematic modeling of the hexapod mechanism. The geometric layout is described and then the kinematic model is derived.

A. Geometric Layout

For convenience, we define the following parameters for describing the geometry of the kinematic model. The length of each strut is denoted as L_i, which is defined as the distance between the centers of the two spherical joints located respectively at the end of the strut A_i and B_i. At the original position of the hexapod mechanism, we denote the positions of the three center points at the top platform and the six at the base stages by A_i^0, and by B_i^0, respectively. L_i^0 is the original length of the strut. Fig. 3 shows the geometrical relationship of the nine points. The top three points are symmetrically placed at the corners of a triangle. The bottom six points are also symmetrically placed at the corners of a hexagon. The variation of the location of the

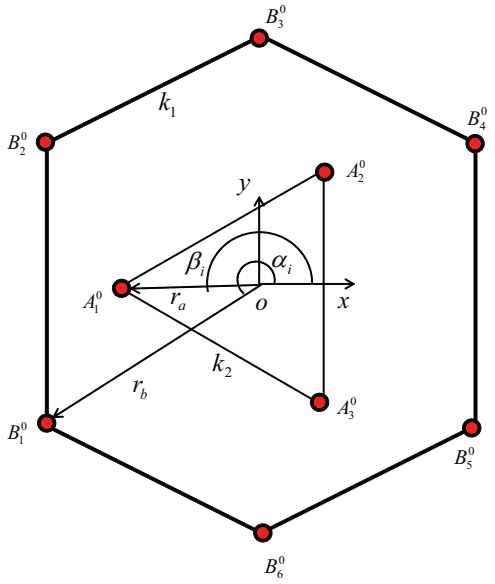

Fig. 3. Geometric Layout of the Joints of the Top Platform and the Bottom Stages.

bottom six points could be polar symmetrical, such as the example shown in Fig. 2. We denote the distance between the intersecting points of the struts at the bottom stage as k_1. For the top platform, the distance between the intersecting points of the struts is k_2. These points on the moving platform and the stages can be described in the global coordinate frame as

$$\begin{aligned} A_i^0 &= [R_z(2\pi/3)] \begin{Bmatrix} r_a \\ 0 \\ -t \end{Bmatrix}, i = 1, \ldots, 6 \\ B_i^0 &= [R_z(\pi/3)] \begin{Bmatrix} r_b \\ 0 \\ -H-t \end{Bmatrix}, i = 1, \ldots, 6 \end{aligned} \tag{1}$$

where $[R(\cdot)]$ is the 3-by-3 rotation matrix about the z axis. H denotes the height between the top surface of the bottom stage and the bottom surface of the top platform. t is the thickness of the top platform. r_a and r_b are the radii of the strut attachment points (bottom plates in home position)[18], [19]. H is the height of the hexapod mechanism from the bottom stage to the top plane of the platform and it is derived as the unknown by solving equation $(A_1^0 - B_1^0)^T(A_1^0 - B_1^0) - L_1^{0\,2} = 0$. t is the thickness of the top platform.

B. Kinematic Model

As shown in Fig. 4, line d_1 is defined as the shortest distance between point A_1 and vector $\overrightarrow{B_1^0 B_2^0}$. Thus, d_1 is perpendicular to $\overrightarrow{B_1^0 B_2^0}$ and the interaction of them is C_1 [17]. As shown in Fig. 5, the vector $\vec{d_1}$ is $\overrightarrow{C_1 A_1}$. Go through C_1, we draw a vector $\vec{e_1}$, which lies in the plane of base stage, and is perpendicular to the z axis of the global frame.In geometric math, $\vec{e_i}$ is defined as

$$\vec{e_i} = \vec{z} \times \vec{u_i}, i = 1, 2, 3 \tag{2}$$

where vector $\vec{u_i}$ is the normalized vector of $\overrightarrow{B_2^0 B_1^0}$,$\overrightarrow{B_4^0 B_3^0}$,$\overrightarrow{B_6^0 B_5^0}$. They are denoted as

ISBN: 978-988-19253-6-7
ISSN: 2078-0958 (Print); ISSN: 2078-0966 (Online)

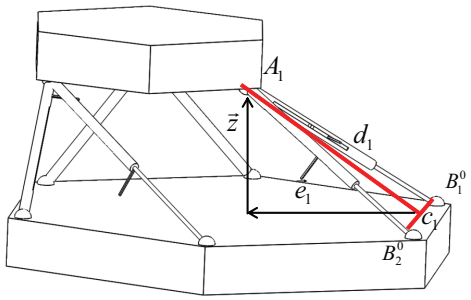

Fig. 4. Kinematic Modeling of the 3-6 Hexapod Mechanism.

$$\begin{aligned}\vec{u}_1 &= \frac{\overrightarrow{B_2^0 B_1^0}}{k_1}\\ \vec{u}_2 &= \frac{\overrightarrow{B_4^0 B_3^0}}{k_1}\\ \vec{u}_3 &= \frac{\overrightarrow{B_6^0 B_5^0}}{k_1}\end{aligned} \tag{3}$$

where vector $\overrightarrow{B_2^0 B_1^0}$ and $\left|\overrightarrow{B_2^0 B_1^0}\right|$ are denoted as

$$\overrightarrow{B_2^0 B_1^0} = \vec{B}_1^0 - \vec{B}_2^0 \tag{4}$$

$$\begin{aligned}k_1 &= \left|\overrightarrow{B_6^0 B_5^0}\right| = \left|\overrightarrow{B_4^0 B_3^0}\right| = \left|\overrightarrow{B_2^0 B_1^0}\right|\\ &= \left(\vec{B}_1^0 - \vec{B}_2^0\right)^T \left(\vec{B}_1^0 - \vec{B}_2^0\right)\end{aligned} \tag{5}$$

The length d_i is defined by the equations

$$\begin{aligned}d_1 &= L_2 Sin\phi_1\\ d_2 &= L_4 Sin\phi_2\\ d_3 &= L_6 Sin\phi_3\end{aligned} \tag{6}$$

where ϕ_i is derived by the k_1 and L_i. L_i denotes the changed length of the strut when the top platform moves to a new position.

$$\begin{aligned}\phi_1 &= ArcCos\left(\frac{k_1^2 + {L_2}^2 - {L_1}^2}{2k_1 L_2}\right)\\ \phi_2 &= ArcCos\left(\frac{k_1^2 + {L_4}^2 - {L_3}^2}{2k_1 L_4}\right)\\ \phi_3 &= ArcCos\left(\frac{k_1^2 + {L_6}^2 - {L_5}^2}{2k_1 L_6}\right)\end{aligned} \tag{7}$$

As shown in Fig. 5, the position of point A_i is derived by a serial chain of vector $\vec{C}_i$, and the projection of $\vec{d}_i$ on $\vec{e}_i$ and $\vec{z}$. $\vec{C}_i$ is the position vector of point C_i in the global coordinate.

$$\vec{A}_i = \vec{C}_i + d_i \vec{z} Sin\psi_i + d_i \vec{e}_i Cos\psi_i \tag{8}$$

where ψ_i is the angle between $\vec{d}_i$ and $\vec{e}_i$. Since the top platform is a rigid body, the distance between two points is a constant. After we obtain the positions of A_i, we can build three constraint equations,

$$\begin{aligned}E_1 &: \left|\overrightarrow{A_2 A_1}\right| - {k_2}^2 = 0\\ E_2 &: \left|\overrightarrow{A_3 A_2}\right| - {k_2}^2 = 0\\ E_3 &: \left|\overrightarrow{A_1 A_3}\right| - {k_2}^2 = 0\end{aligned} \tag{9}$$

where $\left|\overrightarrow{A_2 A_1}\right| = (\vec{A_1} - \vec{A_2})^T (\vec{A_1} - \vec{A_2})$.

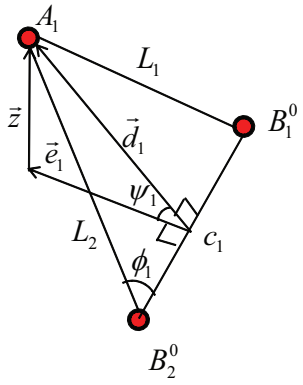

Fig. 5. Derivation of the Kinematic Model.

IV. MEASUREMENT ALGORITHM

In this section, we present the measurement algorithm based on the forward kinematics.

A. Forward Kinematics

Regarding the modeling of the parallel mechanisms, it is easier to obtain the inverse kinematic solution than the forward kinematic solution. In the inverse kinematics, the position of the top platform is the input and the output is the lengths of the struts. In the forward kinematics, we try to obtain the position of the top platform in 6DOF given the lengths of the struts.

In the forward kinematics, the output is the displacement of the top platform which is given by a 4 by 4 transformation matrix $[T]$, further defined by a rotation matrix $[R]$ and a vector $\vec{v}$. The transformation matrix $[T]$ is unknown while the lengths are known values in the forward kinematics. However, they are governed by the constraint Eq. (9). After solving Eq. (9) for ψ_i, we can obtain the positions of the spherical joints of the top platform at the new position by substitute ψ_i into Eq. (8). The vector $\vec{v}$ is derived by the center of the three points.

$$\vec{v} = \frac{\sum_i^3 \vec{A}_i}{3} \tag{10}$$

The rotation matrix $[R]$ is

$$[R] = \left([A_1 A_2 A_3] - [v\ v\ v]\right)\left[A_1^0 A_2^0 A_3^0\right]^{-1} \tag{11}$$

B. Rotation Matrix

As we all know, the rotation matrix can be obtained by the product of three rotation matrices $[R_x(\theta_x)], [R_y(\theta_y)], [R_z(\theta_z)]$. Based on the sequence of the rotation about the axes, we could obtain 6 combinations.

$$\begin{aligned}[R] = &[R_x][R_y][R_z], \quad [R_x][R_z][R_y],\\ &[R_y][R_x][R_z], \quad [R_y][R_z][R_x],\\ &[R_z][R_x][R_y], \quad [R_z][R_y][R_x].\end{aligned} \tag{12}$$

We can derive the rotational angles $\theta_x, \theta_y, \theta_z$, in the forward kinematics given the derived $[R]$ and the sequence of the rotations.

Furthermore, the rotation of a coordinate can also be defined by the Tait-Bryan angles with yaw, pitch, and roll.

ISBN: 978-988-19253-6-7
ISSN: 2078-0958 (Print); ISSN: 2078-0966 (Online)

Here, we denote them as $\theta_Y, \theta_P, \theta_R$, respectively. In order to build the relationship between the rotation matrix and angles, we define the rotation matrix in a general way with 9 elements.

$$[R] = \begin{bmatrix} a_{11} & a_{12} & a_{13} \\ a_{21} & a_{22} & a_{23} \\ a_{31} & a_{32} & a_{33} \end{bmatrix} \tag{13}$$

The angles $\theta_Y, \theta_P, \theta_R$ are governed by 3 equations.

$$\begin{aligned} a_{11} &= Cos\,(\theta_Y) \\ a_{22} &= Cos\,(\theta_P) \\ a_{33} &= Cos\,(\theta_R) \end{aligned} \tag{14}$$

Due to the property of the rotation matrix, the elements are also governed by 6 constraint equations.

$$\begin{aligned} {a_{11}}^2 + {a_{21}}^2 + {a_{31}}^2 &= 1 \\ {a_{12}}^2 + {a_{22}}^2 + {a_{32}}^2 &= 1 \\ {a_{13}}^2 + {a_{23}}^2 + {a_{33}}^2 &= 1 \\ a_{13} &= a_{21}a_{32} - a_{22}a_{31} \\ a_{23} &= a_{31}a_{12} - a_{32}a_{11} \\ a_{33} &= a_{11}a_{22} - a_{12}a_{21} \end{aligned} \tag{15}$$

Given the rotation matrix $[R]$, we can also obtain the angles $\theta_Y, \theta_P, \theta_R$ based on Eq. (14) in the forward kinematics. However, due to the range of the Cosine function, multiple solutions will be obtained. Thus, we need Eq. (15) to further evaluate the solutions. Multiple solutions are introduced also because of the potential symmetrical layout of the mechanism. It is undetermined if the values of the strut lengths are the only given information. Some more information or assumptions are needed to determine the positions and angles. For example, if the platform is used to continuously measure small displacements, we can apply the minimum energy method to find the unique solution.

C. Motion Measurement of Forward Kinematics

The measurement algorithm of the forward kinematics is illustrated in the flowchart of Fig. 6. Here, δ_i^e are the known values. $\left(\theta_x^e, \theta_y^e, \theta_z^e\right)$ or $\left(\theta_Y^e, \theta_P^e, \theta_R^e\right)$ and $\vec{v}^e$ are unknowns. We try to calculate the error of the rotational displacements and the error of the translational displacements $\vec{\mu}$.

1) Record the measurement data δ_i^e of the changed lengths of the struts.
2) Calculate the total strut length L_i^e.

$$L_i^e = L_i^0 + \delta_i^e \tag{16}$$

3) Substitute L_i as L_i^e, and build the forward kinematic model by Eq. (1)-(8).
4) Solve Eq. (9) for ψ_i.
5) Calculate $\vec{A}_i$ by substitute the solutions obtained from step 4 to Eq. (8).
6) Derive $[R^e]$ and $\vec{v}^e$ from $\vec{A}_i$ by Eq. (10) and Eq. (11).
7) Determine the rotational angles of the measurement object: $\theta_x^e, \theta_y^e, \theta_z^e$ or $\theta_Y^e, \theta_P^e, \theta_R^e$.
8) Calculate $\theta_x^e, \theta_y^e, \theta_z^e$ by solving Eq. (12).
   Or calculate $\theta_Y^e, \theta_P^e, \theta_R^e$ by Eq. (14).
9) Obtain the ideal target rotational angles of the object: $\theta_x, \theta_y, \theta_z$ or $\theta_Y, \theta_P, \theta_R$.
   Obtain the target translational displacement of the object $\vec{v}$.

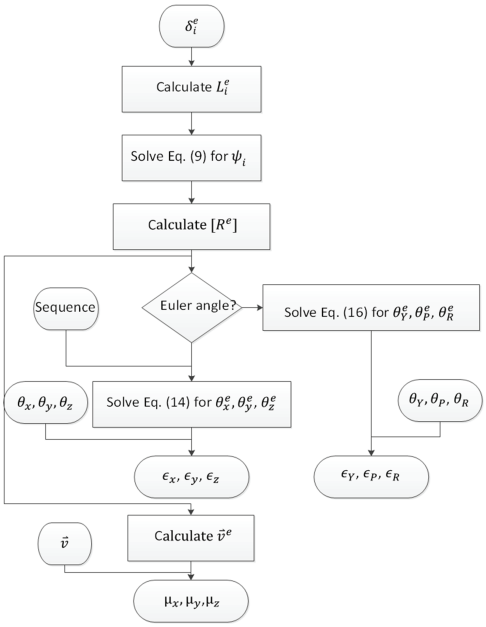

Fig. 6. Measurement Algorithm of Forward Kinematics.

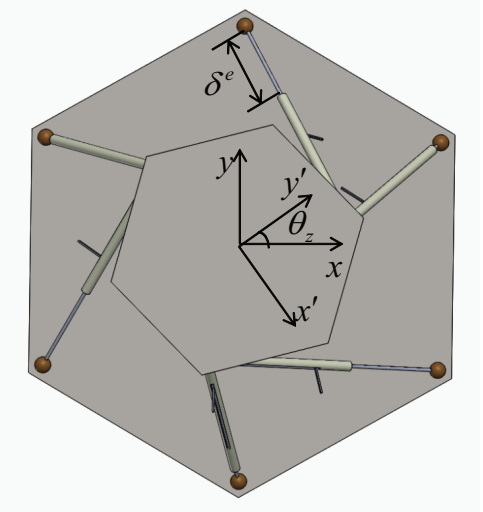

Fig. 7. Pure Rotation along z Axis.

10) The errors of the rotational displacement are calculated by

$$\epsilon = \theta - \theta^e \tag{17}$$

where ϵ includes $\epsilon_x, \epsilon_y, \epsilon_z$ or $\epsilon_Y, \epsilon_P, \epsilon_R$.

11) The errors of the translational displacement are calculated by

$$\vec{\mu} = \left\{ \begin{array}{c} \mu_x \\ \mu_y \\ \mu_z \end{array} \right\} = \vec{v} - \vec{v}^e \tag{18}$$

V. CASE STUDY AND DISCUSSION

An example of the pure rotation along the z axis is shown in Fig. 7. Assume that the platform is targeted to purely rotate with an angle θ_z, our goal is to measure the motion accuracy of the target object.

In the forward kinematic measurement algorithm, the error is calculated by Eq. (17).

ISBN: 978-988-19253-6-7
ISSN: 2078-0958 (Print); ISSN: 2078-0966 (Online)

$$\epsilon_z = \theta_z - \theta_z^e \tag{19}$$

The discussion of the measurement algorithm is shown as following:

1) Forward kinematic algorithm directly shows the errors in 6DOF. The case study shows that it can evaluate the measurement according to the single DOF.
2) In the forward kinematics, we firstly need the measurement data and then do a series of calculation based on the data. For example, the target object is programmed to move to a list of ideal target positions. The hexapod sensor follows the object movements and records a list of real data, δ_i^e. Based on the real data, we derive the real positions. The target real experimental positions and the ideal target positions can be used to calculate the errors.
3) In the inverse kinematics, we can calculate the theoretical solution δ_i before the measurement. For example, a list of the target positions is created. Based on the list, we calculate a list of δ_i before the measurement. During the measurement, we can calculate the error immediately after obtaining the measurement data. This efficient algorithm can also be programmed to a real-time algorithm.
4) Both algorithms require calculation of rotation matrix and translational vector, however the calculation is done in the different steps.
5) According to the requirement of the measurement, we choose the appropriate algorithm.

VI. CONCLUSION

In this paper, we present a design of a 3-6 hexapod platform sensor for measuring the displacements in 6DOF. An analytical model is described based on the geometric layout and kinematic modeling of the mechanism. Based on the forward kinematics, we derive a measurement algorithm according to two angles systems for the hexapod platform sensor. A case study and discussion are proposed for the application of the sensor, and the appropriate choice of the measurement algorithms according to the different situations.

REFERENCES

[1] H.-J. Su, H. Shi, and J. Yu, "A symbolic formulation for analytical compliance analysis and synthesis of flexure mechanisms," *ASME Journal of Mechanical Design*, vol. 134, no. 5, p. 051009, 2012.
[2] H. Shi and H.-J. Su, "An analytical model for calculating the workspace of a flexure hexapod nanopositioner," *ASME Journal of Mechanisms and Robotics*, vol. 5, no. 4, p. 041009, 2013.
[3] Q. Xu, "New flexure parallel-kinematic micropositioning system with large workspace," *Robotics, IEEE Transactions on*, vol. 28, no. 2, pp. 478–491, April 2012.
[4] Y. Li and Q. Xu, "A totally decoupled piezo-driven xyz flexure parallel micropositioning stage for micro/nanomanipulation," *Automation Science and Engineering, IEEE Transactions on*, vol. 8, no. 2, pp. 265–279, April 2011.
[5] H. Shi, X. Duan, and H.-J. Su, "Optimization of the workspace of a MEMS hexapod nanopositioner using an adaptive genetic algorithm," in *Robotics and Automation (ICRA), 2014 IEEE International Conference on*, May 2014, pp. 4043–4048, hong kong, May 31-June 7.
[6] M. L. Culpepper and G. Anderson, "Design of a low-cost nanomanipulator which utilizes a monolithic, spatial compliant mechanism," *Precision Engineering*, vol. 28, no. 4, pp. 469 – 482, 2004.
[7] S.-C. Chen and M. L. Culpepper, "Design of a six-axis micro-scale nanopositionerhexflex," *Precision Engineering*, vol. 30, no. 3, pp. 314 – 324, 2006.
[8] N. G. Dagalakis, J. S. Albus, B.-L. Wang, J. Unger, and J. D. Lee, "Stiffness study of a parallel link robot crane for shipbuilding applications," *Journal of Offshore Mechanics and Arctic Engineering*, vol. 111, no. 3, pp. 183–193, 1989.
[9] D. Chao, G. Zong, R. Liu, and J. Yu, "A novel kinematic calibration method for a 3DOF flexure-based parallel mechanism," in *Proceeding of 2006 IEEE/RSJ International Conference on Intelligent Robots and Systems*. IEEE, Oct. 2006, pp. 4660–4665.
[10] K. M. Varadarajan and M. L. Culpepper, "A dual-purpose positioner-fixture for precision six-axis positioning and precision fixturing: Part i. modeling and design," *Precision Engineering*, vol. 31, no. 3, pp. 276 – 286, 2007.
[11] H. Shi, H.-J. Su, N. Dagalakis, and J. A. Kramar, "Kinematic modeling and calibration of a flexure based hexapod nanopositioner," *Precision Engineering*, vol. 37, no. 1, pp. 117 – 128, 2013.
[12] J.-S. Chen and W.-Y. Hsu, "Design and analysis of a tripod machine tool with an integrated cartesian guiding and metrology mechanism," *Precision Engineering*, vol. 28, no. 1, pp. 46 – 57, 2004.
[13] H. Shi and H.-J. Su, "Workspace of a flexure hexapod nanopositioner," in *Proceedings of ASME IDETC/CIE*, 2012, chicago, Illinois, August 12-15.
[14] H.-J. Su, H. Shi, and J. Yu, "Analytical compliance analysis and synthesis of flexure mechanisms," in *Proceedings of ASME IDETC/CIE*, 2011, washington, DC, August 28-31.
[15] A. Olarra, J. Allen, and D. Axinte, "Experimental evaluation of a special purpose miniature machine tool with parallel kinematics architecture: Free leg hexapod," *Precision Engineering*, vol. 38, no. 3, pp. 589 – 604, 2014.
[16] A. Nubiola and I. A. Bonev, "Absolute robot calibration with a single telescoping ballbar," *Precision Engineering*, vol. 38, no. 3, pp. 472 – 480, 2014.
[17] P. Nanua, K. Waldron, and V. Murthy, "Direct kinematic solution of a stewart platform," *Robotics and Automation, IEEE Transactions on*, vol. 6, no. 4, pp. 438–444, Aug 1990.
[18] H. Shi, H.-J. Su, and N. Dagalakis, "A stiffness model for control and analysis of a MEMS hexapod nanopositioner," *Mechanism and Machine Theory*, vol. 80, pp. 246 – 264, 2014.
[19] H. Shi, "Modeling and analysis of compliant mechanisms for designing nanopositioners," Ph.D. dissertation, The Ohio State University, Columbus, OH,USA, 2013.

ISBN: 978-988-19253-6-7
ISSN: 2078-0958 (Print); ISSN: 2078-0966 (Online)